Prediction of Viscoelastic Behavior of Interphase in Polypropylene-Chopped Rice Husk Composites for β-Relaxation Domain

Amir Ershad-Langroudi, Mohammad Razavi-Nouri, Abdulrasoul Oromiehie

Iran Polymer and Petrochemical Institute, P.O. Box 14965/115, Tehran, Iran

Received 23 August 2009; accepted 23 August 2010
DOI 10.1002/app.33281
Published online 1 December 2010 in Wiley Online Library (wileyonlinelibrary.com).

ABSTRACT: The effect of chopped rice husk (CRH) content on viscoelastic properties and crystallinity of polypropylene (PP) composites was investigated. Composites containing 0, 20, and 40 part per hundred plastics (php) of CRH into PP were prepared by twin-screw extruder, with maleic anhydride-grafted PP as the coupling agent. The viscoelastic behavior and the crystallinity of these composites have been studied by dynamic mechanical analysis as well as differential scanning calorimetry, respectively. By the incorporation of CRH into PP, the storage modulus (E') was found to be increased progressively, whereas the mechanical loss factor (tan δ) decreased in a nonlinear manner. A self-consistent analysis was proposed for the prediction of viscoelastic response of the interphase between PP matrix and CRH particles. A three-phase model was applied in a reverse mode, and the viscoelastic behavior of the interphase was extracted and compared with the unfilled matrix. Differential scanning calorimetry results indicated that CRH influences crystallization temperature as well as the degree of crystallinity of the composites. An entrapped polymer within CRH filler and PP matrix was detected by scanning electron microscope, which can be attributed to the interfacial layer with a good adhesion between the main components. © 2010 Wiley Periodicals, Inc. J Appl Polym Sci 120: 1642–1651, 2011

Key words: composites; mechanical properties; thermal properties; poly(propylene) (PP); simulations

INTRODUCTION

Natural fiber polymer composites are widely used for various applications. In recent years, the addition of agro wastes to thermoplastic polymers has been spread because of the economical reasons and biodegradability.[1] However, natural fibers exhibit a high moisture absorption, which can be a limitation for their processing with other materials; therefore, drying of natural fibers before compounding is very important.[2] It has also been found that predrying of piassava fibers can be an effective factor to improve the flexural strength of polyester composites. The flexural strength of the composite containing 40 (wt %) of the as-received piassava fibers at two different molding forces of 0 and 15 Ton were reported to be 55.4 ± 7.4 and 71.8 ± 3.4 MPa, respectively. The results also revealed that the flexural strength improved as much as 75% when the composite was prepared using the dried fiber, independent of the molding force exerted during the sample preparation.[2]

Rosa et al.[3] studied the water absorption of polypropylene (PP) composites containing 10–40 wt % of rice husk flour (RHF) with time. They reported that water absorption of the composites greatly increased with RHF concentration, and the composite containing 40 wt % of RHF absorbed 11 wt % of water after being immersed for 400 h.

The effects of water absorption on the mechanical properties were also studied for hemp fiber-reinforced unsaturated polyester composites. It was found that water uptake increased with increase in the volume fraction of fiber because of the increase in voids and cellulose content. It was also reported that the tensile and flexural properties of the composites decreased significantly after the composite remained 30 min in boiling water. This was attributed to the degradation of the fiber–matrix interface.[4]

The other drawback of using natural fibers as reinforcing materials in polymer-based composites is their poor interfacial adhesion and low degree of dispersion in the matrix.[5] Similar to all other composites, the mechanical properties of natural fiber composites not only depend on fiber properties but also on the adhesion between natural fiber and the polymer used.[6] Using coupling agents can increase the interfacial adhesion between the components. Therefore, coupling agents play an important role in the final properties of polymer composites.[7–14]

The physical and mechanical properties of the PP/wood flour (WF) composites containing coupling

Correspondence to: A. Ershad-Langroudi (A.Ershad@ippi.ac.ir).

agent such as PP modified with an organosilane compound or maleic anhydride have been investigated and compared with those of the reference composites (without coupling agent). It was observed that both coupling agents improved the tensile properties as well as water absorption content of the composites. However, it is worth to mention that the composites containing PP-organosilane compound show higher tensile strength, lower level of water absorption, and more homogeneous morphology than those containing maleic anhydride. The thermal stability of the composites containing one of the two coupling agents were also similar but higher than that of the reference composite.[15]

Compounding of natural fiber with a polymer matrix affects the thermal and mechanical properties of the composite produced.[16–20] It is found that chopped rice husk (CRH) fibers have some influences on the crystallization of PP.[16] Studies of the thermal properties of CRH-filled PP showed that the thermal stability, storage modulus, and loss modulus of the composites were slightly improved with increasing maleic anhydride-grafted PP (MAPP) as a coupling agent. However, the melting temperatures of the composites were not significantly changed. This enhancement in thermal stability and other properties could be attributed to an improvement in the interfacial adhesion and compatibility between CRH and the matrix.[19]

Nuñez et al.[21] have studied the thermal and dynamic mechanical characteristics of PP-WF composites. They have reported that the composite containing MAPP shows slightly higher storage shear modulus at low temperature than that of the WF composite prepared without any coupling agent. This behavior has been attributed to the attachment of the MAPP to the WF surface, which can also form entanglements with the PP molecular chains.

Dynamic mechanical and thermal properties of modified PP-wood fiber composites have been studied by Hristov and co-workers.[18,22,23] This study shows that tan δ peak temperature is higher in the composite with coupling agent compared with the composite that has no treatment.[18] This is in agreement with the improvement of adhesion and interaction between PP matrix and wood fibers. The storage modulus (E') of the composites containing MAPP was also higher than those of the ones without coupling agent at low temperatures (up to the β-relaxation). In the temperature range from β-transition to 60°C, the composites incorporated with MAPP showed lower modulus, and, above this range, the E'-T curves tended to converge. Thermal properties of the composites also indicated that the wood fibers could act as nucleating agents, whereas MAPP slightly retarded the crystallization rate of PP. The study of morphology of the composite containing MAPP revealed that it was composed mainly of large spherulites with a higher degree of crystallinity compared with that of the uncompatibilized composite.[18]

Many authors have tried to simulate the viscoelastic properties of high filled particulate composites by taking into account the change in morphological feature of nonuniform distribution of filler and reinforced zone in the matrix.[24–30] Gauthier et al.[24] have simulated the dynamic mechanical behavior of unidirectional composites including 43–68% of E-glass fibers in an epoxy matrix based on successive applications of the three-phase self-consistent analysis proposed originally by Christensen and Lo.[31] The effect of nonuniform distribution of the glass fiber in the matrix and lower mobility of the macromolecules in the vicinity of the filler (i.e., the polymer in the interphase) were considered by them for the simulation.[24]

In another study, the dynamic mechanical behavior of epoxy/A-glass bead composites was investigated considering the influence of the volume fraction of the beads and their surface treatments. The self-consistent analysis was also used to calculate the effective shear modulus of the composite with spherical inclusions.[25]

Albérola and co-workers[28–30] proposed the mechanical models that can predict the reinforcing effect of polymeric composites by particulates as well as unidirectional fibers over wide range of volume fraction of fillers and temperatures (or frequencies). These approaches are based on both the definition of a representative morphological pattern (RMP), accounting for the presence of fiber clusters, and a quantitative morphology analysis, based on the percolation concept. This approach is extended to describe the viscoelastic properties of a semicrystalline polymer, commingled with unidirectional glass fibers. It was found that aggregates act as the continuous phase. Based on the use of a mechanical model in a reverse mode, the actual viscoelastic behavior of the transcrystalline region is extracted and compared with that displayed by the unfilled polymer.

After a careful literature review, it can be concluded that the interphase layer plays a major role in determining the mechanical properties of the composite materials. Such results could be of great importance both for the design purposes and for the plastic processing industry. Therefore, the main goal of this work was to analyze the dynamic mechanical behavior and thermal properties of PP composites containing MAPP and various CRH content and also to characterize the viscoelastic behavior of the interfacial layer.

EXPERIMENTAL

Materials

The PP homopolymer was supplied by Bandar Imam Petrochemical Co., Iran, as the grade Poliran

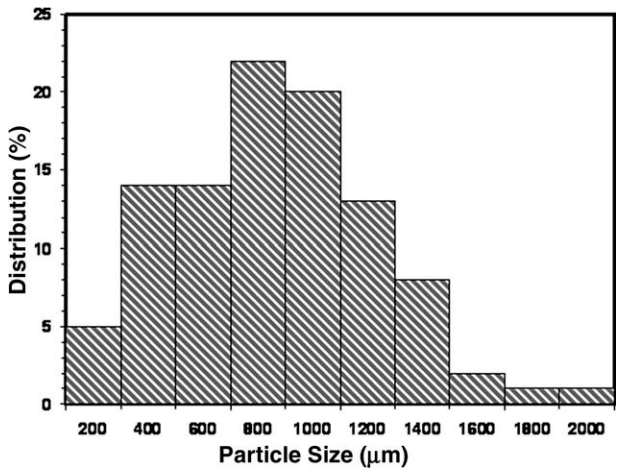

Figure 1 Particle size distribution of CRH.

PI0800 and with the melt flow index of 8 g/10 min. MAPP with melt flow index of 450 g/10 min (190°C and 2.16 kg) was obtained from DuPont as the grade Fusabond MD353D and used as a coupling agent. Irganox 1010 supplied from Ciba was also added into the composites as a heat stabilizer. CRH was obtained from a local rice milling plant, and, after drying in air, was ground in a Wieser grinding machine (WG-LS 200/200). The size distribution of CRH is shown in Figure 1. The average size, in diameter, was found to be 750 ± 250 μm. As we have reported earlier,[32] studies carried out on the morphology of CRH showed that a large number of knobs existed on the outer surface of the virgin CRH. Hair-like structures were also seen in the gaps between the ridges in some regions. However, rather smooth region with no knobs on the surface was observed for the inner part of the CRH.

Sample preparation

Before preparing the composites, CRH particles were dried at 105°C for 24 h to remove moisture. Composites including three different amounts of CRH (i.e., with 0, 20, and 40 php) were prepared by using a Brabender Plasticorder model DSE 20 twin-screw extruder. The screws with a 20-mm diameter and a 40 : 1 length/diameter ratio were used, and the screw speed was 130 rpm. The MAPP, Irganox 1010, and calcium carbonate ($CaCO_3$) content in the recipe for the preparation of PP/CRH composites were kept constant. The ratio of MAPP, Irganox 1010, and $CaCO_3$ were 3, 0.1, and 3 wt % of the polymer content, respectively. The reference sample was made of PP and all the other ingredients except CRH. To make the composites, PP and other ingredients were thoroughly mixed in a tumble blender and fed into the twin-screw extruder by using a forced feeder. Degassing was also accomplished during extrusion via a vacuum pump. The venting zone was located at the fourth zone out of five near to the die region. The temperature of five different barrel zones and the die were set to 165, 185, 215, 210, 195, and 185°C, respectively. The output of extruder was formed as the pellets and dried at 120°C for 24 h before compression molding. Square plaques (150 mm × 150 mm × 2 mm) were obtained by pressing the extruded pellets between PTFE sheets using a Toyoseiki hydraulic press (model MP-S). The press plates were maintained at 190°C, and molding was carried out at two different stages. First, the hot mold was filled with pellets, and the plates were then slowly closed within 2 min to facilitate flowing of material into the mold. Subsequently, the pellets were compressed for 1 min at a pressure of 25 MPa. The mold was then cooled to room temperature, and the specimen was removed from the press. The matrix, the reference sample, and the composites reinforced with 20 and 40 php of CRH particles will be referred to as PP, REF, 20CRH, and 40CRH in this work, respectively.

Differential scanning calorimetry

A Polymer Laboratories differential scanning calorimeter was used for investigating the thermal behavior of the composites. Each sample of 8 ± 1 mg was taken from the molded sheet and enclosed in an aluminum pan. An empty aluminum pan was also used as a reference. Thermal studies were carried out in the temperature range 40–230°C at a heating rate of 10°C/min under nitrogen atmosphere (20 cm^3/min). In the first run, the samples were heated to 230°C and maintained at this temperature for 10 min to eliminate any thermal history. They were then cooled until they reached ambient temperature, at the cooling rate of 10°C/min. In the second run, the samples were reheated up to 230°C at the same heating rate. The thermograms were recorded as a function of temperature.

Dynamic mechanical analysis

Dynamic mechanical analysis (DMA) experiments were carried out by means of a Polymer Laboratories dynamic mechanical thermoanalyzer. Rectangular specimens were subjected to oscillating three-point bending loading. Test specimens with 50 mm × 10 mm × 2 mm dimensions were cut from the compression-molded plates. All measurements were performed at a frequency of 3 Hz, at a heating rate of 1°C/min, and a temperature in the range of −120°C to 120°C. The viscoelastic properties such as E' and tan δ were recorded as a function of temperature.

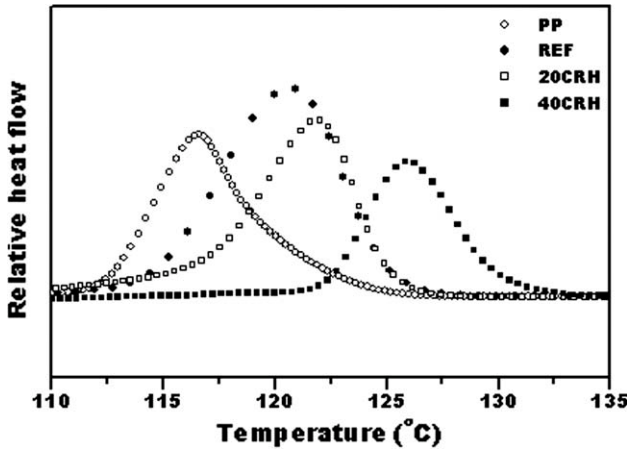

Figure 2 Crystallization exotherms of PP, REF, and the composites.

Scanning electron microscopy

The morphology of the fracture surface of each composite was studied by using a Cambridge scanning electron microscope (model S360) to study the adhesion between CRH filler and matrix as well as any possible agglomeration of CRH in the composite containing 40 php of CRH. The fracture surfaces were prepared by snapping the composites into half at liquid nitrogen temperature. The samples were mounted on the sample stub, and the surface was sputtered with gold.

RESULTS AND DISCUSSION

Thermal properties

The thermal properties and crystallization behavior of PP and the composites were analyzed using nonisothermal differential scanning calorimetry (DSC) experiments. The crystallization exotherms and the second run of the melting endotherms of all the materials studied are shown in Figures 2 and 3, respectively. Melting point was considered as the temperature at which the last trace of crystallinity disappeared.[33] The degree of crystallinity (X_c) was also calculated using the following equation from the second heating run endotherms[34]

$$X_c = \frac{\Delta H_f}{(1-\varphi)\Delta H_f^0} \quad (1)$$

where $1 - \varphi$ is the weight fraction of the polymer, ΔH_f is the enthalpy of melting, and ΔH_f^0 is the theoretical enthalpy value for a 100% crystalline PP, which is taken to be 209 J/g.[35]

Melting temperature (T_m), crystallization temperature (T_c), and the degree of crystallinity are tabulated in Table I. As it is observed, T_c increases for the composite as well as the reference sample compared with that of PP. This can be attributed to the effect of $CaCO_3$ in the reference sample and the influence of both of $CaCO_3$ and CRH in the composites, which act as nucleating agents in the PP matrix. It can also be seen that the degree of crystallinity of PP increases in the reference sample and the composites compared with that of the pristine polymer. However, X_c of the composites is slightly lower than that of the reference sample. Hristov and Vasileva[18] have reported that wood fibers increase the crystallization temperature of composite and they related that to the nucleating activity of the matrix–fiber interface. However, the addition of compatibilizer had a decreasing effect on T_c compared with that of the unmodified PP wood fiber. This observation can be attributed to the restriction of the molecular mobility near the wood surface, which suppresses the nucleating ability.[18] These could be related to the possible modification of the polymer at the vicinity of fillers (e.g., the presence of an interfacial layer).

TABLE I
Thermal Properties of PP, REF, and the Composites

Materials	CRH filler content (php)	T_m (±2°C)	T_c (±2°C)	X_c (±3%)
PP	0	179.1	116.1	24.2
REF	0	176.8	120.9	36.9
20CRH	20	179.3	122.0	33.4
40CRH	40	177.7	125.8	30.6

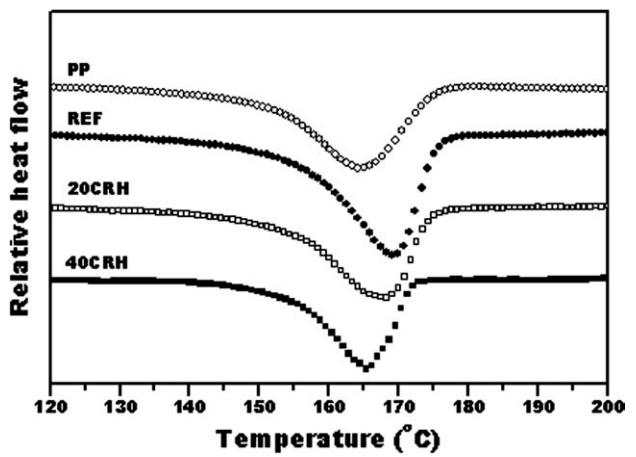

Figure 3 Melting endotherms of PP, REF, and the composites.

Morphology of composites

Scanning electron microscopy examination of 20CRH composite has confirmed a good interaction and adhesion between the PP matrix and CRH particles. Figure 4 shows that an interfacial polymer layer formed around the CRH particles. As can be seen in

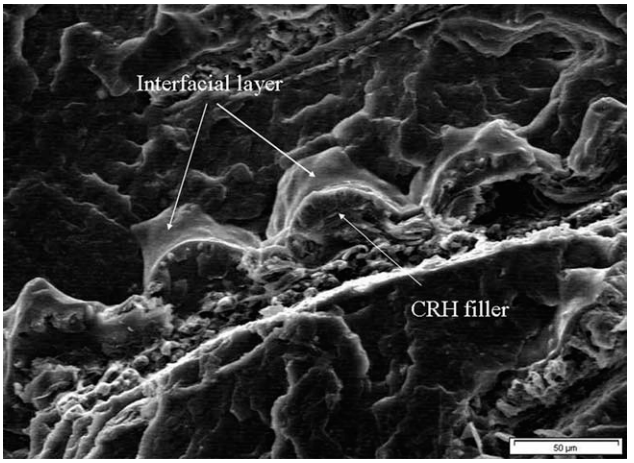

Figure 4 Scanning electron microscopy observation of 20CRH composite.

this figure, the roughness of CRH and MAPP compatibilizer can be responsible for producing a cog-wheel-like grafting on the CRH surface, which is favorable for entanglements with PP chains.[18,36] Good physical interlocking and chemical interaction between MAPP and the particles restrict the molecular mobility near to the CRH surface, and this suggests that the interfacial layer of polymer that is in contact with the CRH particles may have different mechanical properties from the rest of the matrix.[18,24]

Figure 5 shows the agglomeration of CRH particles within 40CRH composite, which can be seen in different locations on the fractured surface. It is observed that the particles are packed as agglomerates within which a part of the polymer is entrapped. With increasing the CRH content from 20 to 40 php in the composites, the possibility of having more agglomeration sites throughout of the composite is increased, and, therefore, the properties of the

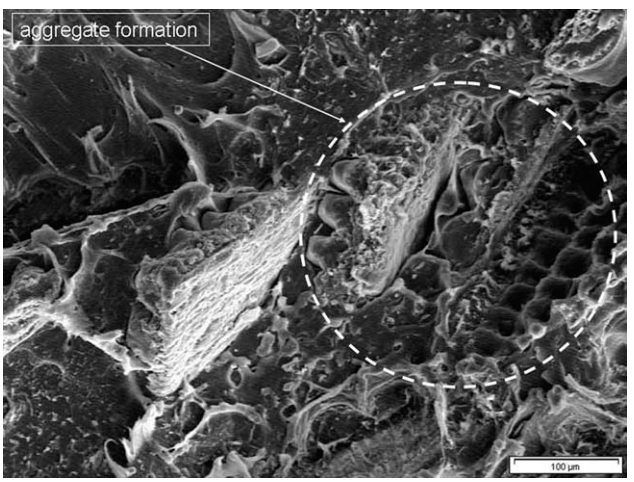

Figure 5 Scanning electron microscopy observation of 40CRH composite and the formation of the aggregates.

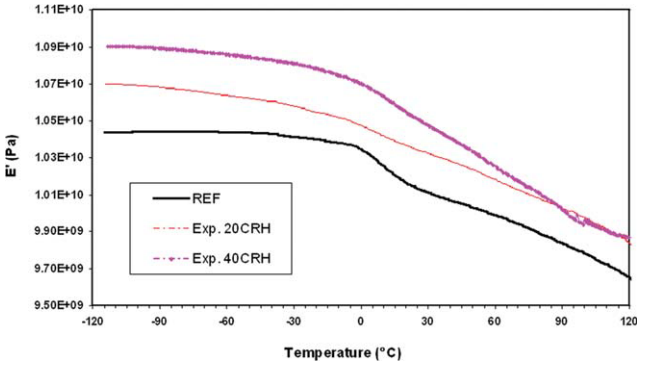

Figure 6 Variation of storage modulus of REF and the composites as a function of temperature at 3 Hz. [Color figure can be viewed in the online issue, which is available at wileyonlinelibrary.com.]

interfacial layer will be changed. In the following parts of the article, both the interphase and occluded polymer are considered as the interfacial layer.

Dynamic mechanical properties

The effects of the filler content on the dynamic mechanical properties of the composites were studied by DMA. The variation of storage modulus as a function of temperature at a frequency of 3 Hz is shown in Figure 6. It is observed that CRH particles have increased the modulus of the composites in the temperature range studied. This can be related to the combination of the effect of the filler embedded in a viscoelastic matrix and the mechanical limitation introduced by CRH at high concentration, which reduces the mobility and deformation of the matrix. Similar results have also been reported by other authors.[37]

It was also found that the storage modulus of the composites decreased with increase in temperature as well as the reference sample. The reduction in storage modulus with temperature occurred because of the polymer matrix softening at high temperature. However, the 40CRH composite showed the highest storage modulus compared with that of the REF and 20CRH. This is expected because the filler incorporated into the polymer has higher modulus than that of the matrix and also the volume fraction of filler in 40CRH is higher than that of 20CRH composite.

Viscoelastic properties of the composites can be evaluated by considering the change in their tan δ values with temperature. Figure 7 shows the experimental variations of tan δ as a function of temperature for the reference sample and the composites. Two peaks can be seen at about 10°C (β-relaxation) and 100°C (α-relaxation) for the reference sample. The transition at lower temperature is attributed to the glass–rubber transition of the amorphous part, whereas the higher one is related to the lamellar slip

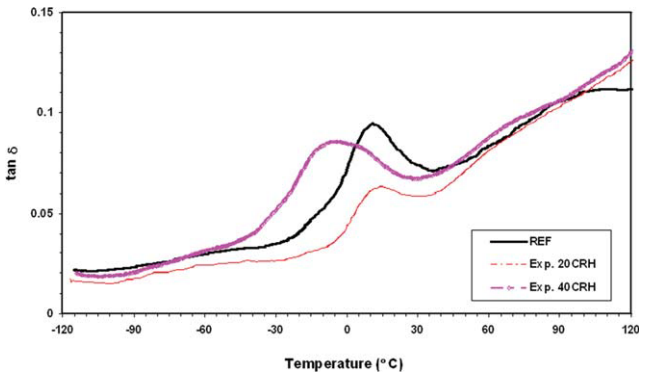

Figure 7 Variation of tan δ of REF and the composites as a function of temperature at 3 Hz. [Color figure can be viewed in the online issue, which is available at wileyonlinelibrary.com.]

and rotation in the crystalline phase of PP.[18,38] However, the origin of α-relaxation is under discussion and attributed to either the presence of defects in the crystalline phase or mechanisms involving both the amorphous and crystalline phases.[26] This figure also shows that the damping factor of the two composites studied is insensitive to the filler content for temperatures greater than 45°C.

The interaction between the polymer and CRH particles at the molecular level affects the position of the primary β-relaxation peak.[18,39] In general, the increase in β-relaxation peak amplitude displays an increase in chain mobility and the amount of amorphous PP chains involved in the transition.[18,40] As Figure 7 illustrates, the β-relaxation temperature of the 20CRH composite is nearly the same to that of the reference sample. This suggests that the amorphous phase in the 20CRH composite behaves very similar to that of REF sample. In addition, the tan δ value decreases with the addition of 20 php CRH into the matrix.

In the case of 40CRH composite, the peak width at half height is higher than those of the reference sample and 20CRH composite. However, the peak height is lower than that of the reference sample, whereas surprisingly is higher than that of the 20CRH composite. The peak width at half height is a criterion used to indicate interaction between the phases and the homogeneity of the amorphous phase. The higher value indicates a better interaction between the phases and a higher heterogeneity of the amorphous phase.[41] The lowering of the peak height and the increase in the peak width at half height of the 40CRH composite (Fig. 7) compared with that of the reference sample can be attributed to the lowering of the mobility of the polymer chains and increased heterogeneity, respectively.

In addition, the increase in the tan δ value and its shifts to lower temperature for the composite containing 40 php CRH compared with 20 php CRH can be attributed to the higher amorphous phase content and lower MAPP/CRH ratio in 40CRH composite than that of 20CRH composite (Table I). It should be noted that MAPP content was constant for all samples studied; thus, the ratio of MAPP to CRH for 40CRH composite was less than that of the 20CRH composite.

The shift in tan δ to higher temperature is an indication of the presence of a process that has restricted the mobility of the chains in the amorphous phase. Therefore, more energy is required for the transition to occur. It has been reported that MAPP restricts the chains motion and increases the β-transition temperature.[42–45] On the other hand, an increase in the intensity or amplitude of the transition reveals that the number of molecular chains that are responsible for this transition to happen has been increased. Thus, it can be concluded that the amorphous content increased by increasing the CRH content in the composites. This unexpected behavior displayed by the 40CRH composite can then be attributed to the following possibilities: (i) some changes in the microstructure of the polymer at the vicinity of CRH fillers is responsible for the increase in molecular motion ability of the chains in the amorphous phase, (ii) the higher heterogeneity of the amorphous phase can be related to the formation of the aggregates of CRH particles, (iii) the higher amorphous phase content in this composite can affect the intensity of β-transition of the pristine polymer, and (iv) the lower MAPP-to-CRH ratio in 40CRH in comparison with that of 20CRH composites can shift the β-relaxation to lower temperature.

Prediction of the viscoelastic behavior of the interphase in β-relaxation domain

In the literature, Christensen and Lo[31] proposed a method for the determination of the effective shear modulus of the composite with spherical inclusions, based on successive applications of the three-phase self-consistent analysis. Recently, this type of approach has been generalized to $(n + 1)$-phase model in the case of n-layered spheres, by Herve and Zaoui[46–48] for isotropic elasticity.

Some authors have applied these models in consecutive steps and taken into account some morphological analysis, including nonuniform arrangement of the particulate fillers in the composite and predicated the viscoelastic behavior of the reinforced polymers by particulates as well as unidirectional fibers over wide ranges of volume fraction of fillers and temperatures. The authors related the changes in the microstructure and the viscoelastic behavior of the polymer at the vicinity of the filler to the development of an interphase.[24–27] The interactions at polymer–filler interface can form an interfacial layer

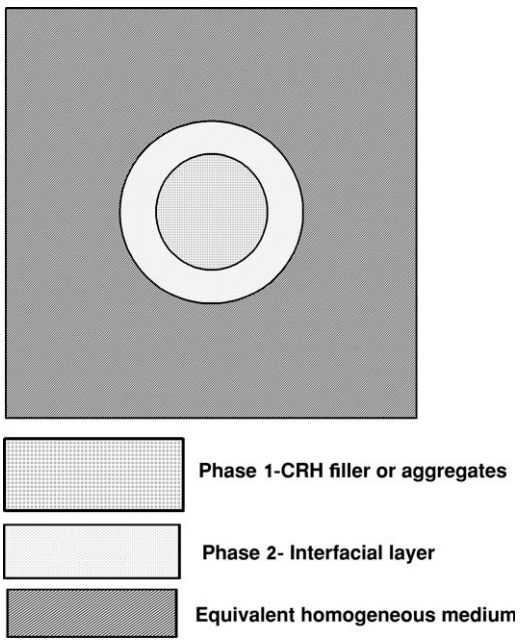

Figure 8 Representative morphological pattern of a three-phase model.

in the vicinity of filler, with properties that are quite different from that of the bulk polymer.

The aim of this section was to predict the viscoelastic behavior of the interphase, by assuming the existence of a well-defined third phase around each particle. This prediction can be performed by using a self-consistent scheme in a reverse mode. The RMP is constituted by a two-layered spherical inclusion in which CRH particle is the central sphere (Phase 1) surrounded by the shell of modified polymer matrix, i.e., an interfacial layer as interphase (Phase 2), embedded in the equivalent homogenous medium as the continuous phase (Fig. 8). Thus, the viscoelastic properties of interphase can be extracted by using Christensen and Lo model in a reverse mode. The knowledge of the viscoelastic behavior of both unmodified polymer matrix and the composite are then required for using this model. In this work, the viscoelastic behavior of unmodified polymer matrix has been considered as the viscoelastic behavior of the reference sample, and the CRH has also been taken as a completely elastic material over the temperature range studied. The tensile modulus of CRH has been extracted from the extrapolation of the composites prepared with different filler weight ratios. The extrapolation showed that the elastic modulus of CRH is about 10 GPa.[49] In the first step, CRH Poisson ratio was considered to be constant and equal to 0.2. The Poisson ratio of the matrix was also assumed to change from 0.32 to 0.4 (the Poisson ratio of the matrix was taken to be 0.32 and 0.4 at $T = 100$ and 473 K, respectively) when the β-relaxation occurs, according to the following equation:

$$\nu_{mj} = 0.32 + 0.08\frac{\log G'_{m(T=100K)} - \log G'_{m(T=Tj)}}{\log G'_{m(T=100K)} - \log G'_{m(T=473K)}} \quad (2)$$

where ν_m and G' are the Poisson ratio and shear modulus of the matrix, respectively, and j is the index of temperature from 100 to 473 K.[25]

Figure 9(a,b) shows the variation of E' and tan δ versus temperature for the interphase and 20CRH composites, respectively. Figure 10(a,b) also illustrate the variation of the same parameters for the interphase and 40CRH, respectively. It was assumed that the mechanical behavior of the interphase is transversely isotropic. In addition, the dynamic mechanical properties of the reference sample are added for comparison in both the figures. As can be observed from Figures 9(a) and 10(a), the storage modulus calculated for the both interphases are significantly greater than that of the reference sample, and its value is higher for the 40CRH than that of the 20CRH composite in the temperature range studied. However, in both cases, the predicted storage modulus for the interphases is lower than that of their composites. It is also worth to mention that Figures 9(b) and 10(b) indicate that the tan δ related to the interphase of the 40CRH composite show a higher and wider relaxation peak, which is located at lower

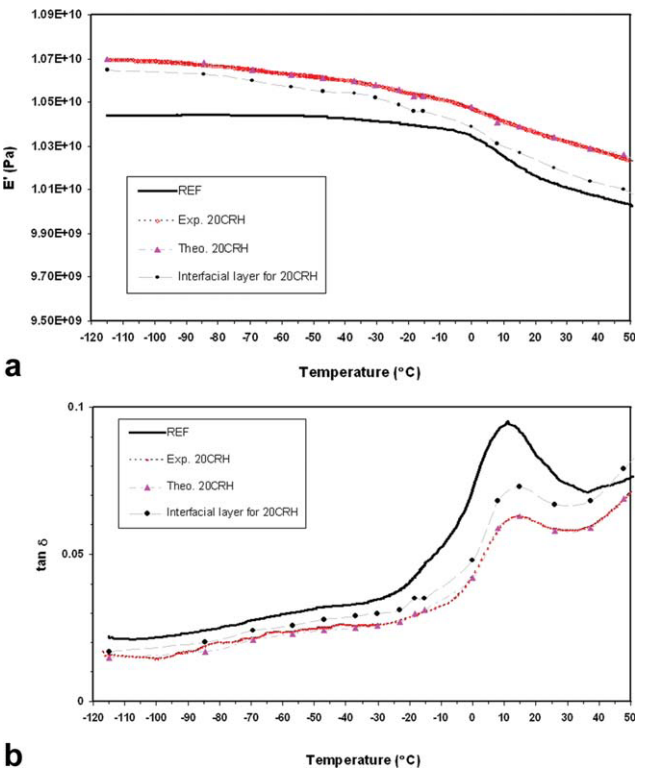

Figure 9 Experimental and theoretical variation of (a) E' and (b) tan δ versus temperature for the REF, 20CRH composite, and its interfacial layer at 3 Hz. [Color figure can be viewed in the online issue, which is available at wileyonlinelibrary.com.]

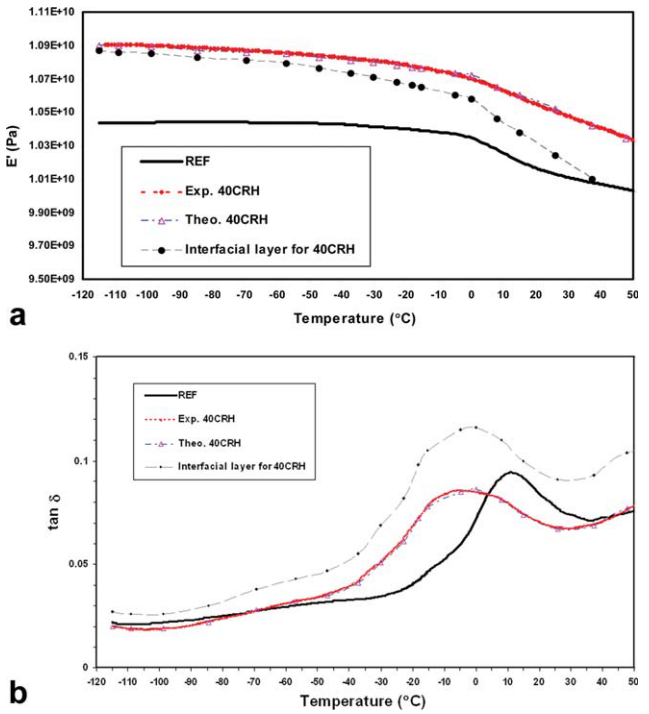

Figure 10 Experimental and theoretical variation of (a) E' and (b) tan δ versus temperature for the REF, 40CRH composite, and its interfacial layer at 3 Hz. [Color figure can be viewed in the online issue, which is available at wileyonlinelibrary.com.]

temperature compared with that of the 20CRH composite.

Accordingly, the viscoelastic properties found for both the interphases confirm the global changes of the crystalline organization of the matrix when the CRH particles are incorporated. This is in agreement with results obtained by DSC. The modifications of the crystalline size and degree of crystallinity, which acts as physical ties, affect the molecular mobility of the amorphous phase of the PP matrix. The results can explain the higher theoretical Young's modulus of the interfacial layer for different composites than that of the bulk polymer.[26,28,50,51] Based on the morphology analysis and the possible aggregate formation, the viscoelastic behavior of the interfacial layer in 40CRH composite has been investigated and compared with that of the 20CRH composite.

Prediction of the viscoelastic behavior of the interphase in the presence of particles aggregates

It is now of interest to calculate the viscoelastic properties of the interfacial layer in the presence of aggregates and in the range β-relaxation occurs. To account for the presence of filler aggregates, the same RMP shown in Figure 8 is also considered for the 40CRH composite. The only difference is that Phase 1 has been replaced by the aggregates as a reinforcing phase.

In the first step, the properties of the aggregates were considered as the properties of the CRH having the critical content of aggregates. It should be mentioned that the maximum volume fraction (Φ_{max}) of the spherical inclusions (aggregate) for a random close packing model is equal to 0.68.[25,52,53] The storage modulus and damping factor for the reference, 40CRH composite, and interfacial layer as a function of temperature are shown in Figure 11(a,b), respectively. For comparison, the above-mentioned [Fig. 9(a)] storage modulus of the interfacial layer calculated for the 20CRH composite has also been added into Figure 11(a). This figure shows that the calculated modulus of the interfacial layer for 20CRH and 40CRH composites are very close to each other below −80°C. However, the modulus of the interfacial layer of the 40CRH composite suddenly decreases above this temperature and has a lower modulus than that of the reference as well as the interfacial layer of the 20CRH composite. Accordingly, it can be concluded that the volume fraction of aggregates is overestimated. Moreover, as observed in Figure 11(b), the experimental and theoretical damping are in agreement with each other.

In the second step, the volume fraction of the aggregates (i.e., Phase 1) was taken to be 30 (vol %),

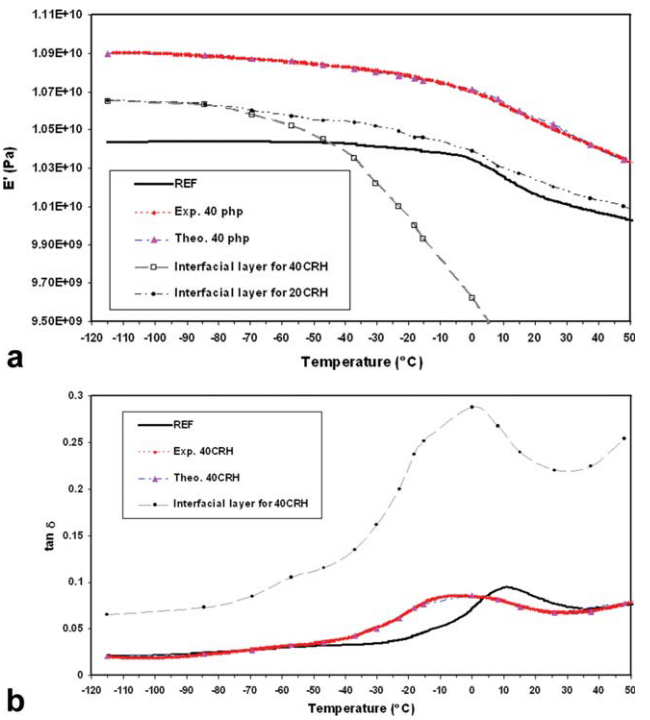

Figure 11 Experimental and theoretical variation of (a) E' and (b) tan δ versus temperature for the REF, 40CRH composite, and the interfacial layers at 3 Hz for $\Phi_{agg} = 68\%$. [Color figure can be viewed in the online issue, which is available at wileyonlinelibrary.com.]

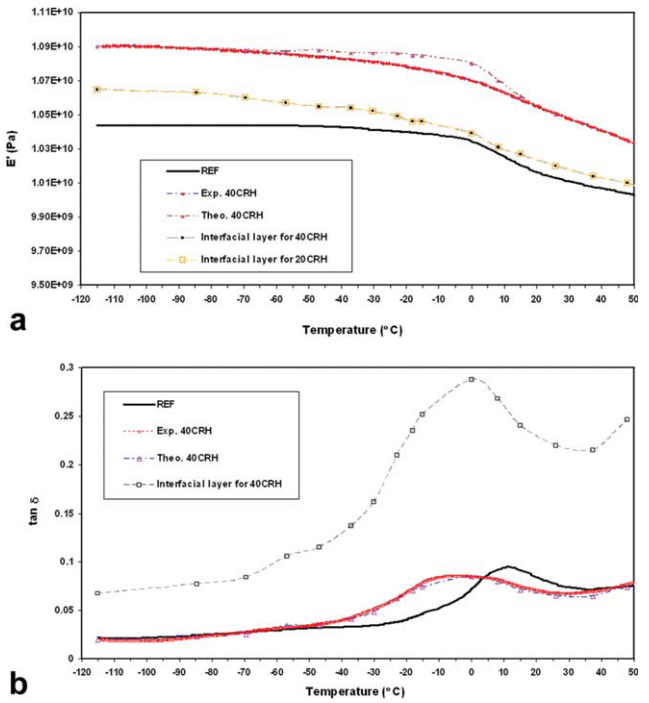

Figure 12 Experimental and theoretical variation of (a) E' and (b) tan δ versus temperature for the REF, 40CRH composite, and the interfacial layers at 3 Hz for $\Phi_{agg} = 30\%$. [Color figure can be viewed in the online issue, which is available at wileyonlinelibrary.com.]

which is slightly more than that of the theoretical volume fraction of CRH in the 40CRH composite (i.e., 26 vol %).[49] The Poisson ratio was also considered to change from 0.2 to about 0.31 according to the following equation:

$$\nu_{aggj} = 0.2 + 0.11\frac{\log G'_{m(T=100K)} - \log G'_{m(T=Tj)}}{\log G'_{m(T=100K)} - \log G'_{m(T=400K)}} \quad (3)$$

where ν_{agg} and G' are the Poisson ratio of aggregates and shear modulus of the matrix, respectively, and j is the index of temperature from 100 to 400 K.

The theoretical behavior of the storage modulus and tan δ of the reference, 40CRH composite, and interfacial layer are depicted in Figure 12(a,b), respectively. The storage modulus of the interfacial layer calculated for the 20CRH composite is also shown in Figure 12(a) for comparison. Good correlations between the results were found by comparing the experimental and theoretical viscoelastic properties of the 40CRH composite. Over the temperature range analyzed, the storage modulus of the interfacial layers calculated for both composites are very close for the aggregate volume fraction of $\Phi_{agg} = 30\%$. This is significantly greater than that of the reference sample. These results indicate that the aggregates of CRH particles act as a reinforcing phase. By comparing Figures 10(b) and 12(b), it can be seen that, by considering the existence of aggregates inside the composite, the amount of amorphous phase increases and, thus, tan δ of the interfacial layer shows a higher peak value.

CONCLUSIONS

The effect of CRH content on the viscoelastic and thermal properties of PP composites were investigated by using DMA and DSC experiments. It was found that the crystallization temperature of the reference sample as well as 20CRH and 40CRH composites increased compared with that of PP. This could be related to the effect of $CaCO_3$ in the reference sample and the influence of both of $CaCO_3$ and CRH in the composites, which act as nucleating agents in the pristine polymer. The degree of crystallinity of PP also increased in the reference sample and the composites compared with that of PP alone. However, the degrees of crystallinities of the composites were slightly lower than that of the reference sample. Based on the possible aggregate formation in the 40CRH composite revealed from morphological analysis, the viscoelastic behavior of the interfacial layer was investigated by using a self-consistent three-phase model (i.e., Christensen and Lo's model) in a reverse mode. The results showed that the storage modulus of the interfacial layer calculated for both composites were very close to each other and significantly greater than that of the reference sample. The change in the location of β-relaxation temperature and its amplitude for the interfacial layer of the 40CRH compared with that of 20CRH composite can also be related to the reduction of the degree of crystallinity and change in the microstructure of the polymer at the vicinity of the CRH particles.

References

1. Rowell, R. M.; Sanadi, A. R.; Caulfield, D. F.; Jacobson, R. E. In Lignocellulosic-Plastics Composites; Leao, A. L., Carvalho, F. X., Frollini, E., Eds.; University of Rio de Janeiro: Rio de Janeiro, 1997; pp 23–51.
2. De Deus, J. F.; Monteiro, S. N.; D'Almeida, J. R. M. Polym Test 2005, 24, 750.
3. Rosa, S. M. L.; Santos, E. F.; Ferreira, C. A.; Nachtigall, S. M. B. Mater Res 2009, 12, 333.
4. Dhakal, H. N.; Zhang, Z. Y.; Richardson, M. O. W. Compos Sci Technol 2007, 67, 1674.
5. Malkapuram, R.; Kumar, V.; Negi, Y. S. J Reinf Plast Compos 2009, 28, 1169.
6. Gauthier, R.; Joly, C.; Coupas, A. C.; Gauthier, H.; Escoubes, M. Polym Compos 1998, 19, 287.
7. Park, B. D.; Wi, S. G.; Lee, K. H.; Singh, A. P.; Yoon, T. H.; Kim, Y. S. Biomass Bioenerg 2004, 27, 353.
8. Toro, P.; Quijada, R.; Murillo, O.; Yazdani-Pedram, M. Polym Int 2005, 54, 730.
9. Panthapulakkal, S.; Sain, M.; Law, S. Polym Int 2005, 54, 137.
10. Zurina, M.; Ismail, H.; Bakar, A. A. J Appl Polym Sci 2004, 92, 3320.
11. Rozman, H. D.; Musa, L.; Abubakar, A. J Appl Polym Sci 2005, 97, 1237.

12. Martí-Ferrer, F.; Vilaplana, F.; Ribes-Greus, A.; Benedito-Borrás, A.; Sanz-Box, C. J Appl Polym Sci 2006, 99, 1823.
13. Panthapulakkal, S.; Law, S.; Sain, M. J Thermoplast Compos 2005, 18, 445.
14. Panthapulakkal, S.; Law, S.; Sain, M. J Appl Polym Sci 2006, 100, 3619.
15. Nachtigall, S. M. B.; Cerveira, G. S.; Rosa, S. M. L. Polym Test 2007, 26, 619.
16. Premalal, H. G. B.; Ismail, H.; Baharin, A. Polym Plast Technol Eng 2003, 42, 827.
17. Ershad-Langroudi, A.; Jafarzadeh-Dogouri, F.; Razavi-Nouri, M.; Oromiehie, A. J Appl Polym Sci 2008, 110, 1979.
18. Hristov, V.; Vasileva, S. Macromol Mater Eng 2003, 288, 798.
19. Kim, H. S.; Kim, S.; Kim, H. J.; Yang, H. S. Thermochim Acta 2006, 451, 181.
20. Kim, H. S.; Yang, H. S.; Kim, H. J.; Park, H. J. J Therm Anal Calorim 2004, 76, 395.
21. Nuñez, A. J.; Kenny, J. M.; Reboredo, M. M.; Aranguren, M. I.; Marcovich, N. E. Polym Eng Sci 2002, 42, 733.
22. Hristov, V. N.; Krumova, M.; Vasileva, St.; Michler, G. H. J Appl Polym Sci 2004, 92, 1286.
23. Hristov, V. N.; Vasileva, St.; Krumova, M.; Lach, R.; Michler, G. H. Polym Compos 2004, 25, 521.
24. Gauthier, C.; Khavandi, A.; Franciosi, P.; Perez, J.; Gaertner, R. Polym Compos 1998, 19, 667.
25. Shaterzadeh, M.; Gauthier, C.; Gerard, J. F.; Mai, C.; Perez, J. Polym Compos 1998, 19, 655.
26. Dubouloz-Monnet, F.; Albérola, N. D.; Mélé, P. J Appl Polym Sci 2006, 99, 3466.
27. Flandin, L.; Vouyovitch, L.; Beroual, A.; Bessede, J. L.; Albérola, N. D. J Phys D Appl Phys 2005, 38, 144.
28. Vendramini, J.; Mélé, P.; Merle, G.; Albérola, N. D. J Appl Polym Sci 2000, 77, 2513.
29. Mélé, P.; Da Silva, C.; Marceau, S.; Brown, D.; De Puydt, Y.; Albérola, N. D. Macromol Symp 2003, 194, 185.
30. Brown, D.; Marcadon, V.; Mélé, P.; Albérola, N. D. Macromolecules 2008, 41, 1499.
31. Christensen, R. M.; Lo, K. H. J Mech Phys Solids 1979, 27, 315.
32. Razavi-Nouri, M.; Jafarzadeh-Dogouri, F.; Oromiehie, A.; Ershad-Langroudi, A. Iran Polym J 2006, 15, 757.
33. Søndergaard, K.; Lyngaae-Jørgensen, J. Rheo-Physics of Multiphase Polymer Systems; Technomic Publishing Co.: Lancaster, 1995.
34. Tjong, S. C.; Bao, S. P. J Polym Sci Part B: Polym Phys 2005, 43, 253.
35. Chen, M.; Tian, G.; Zhang, Y.; Wan, C.; Zhang, Y. J Appl Polym Sci 2006, 100, 1889.
36. Felix, J. M.; Gatenholm, P. J Appl Polym Sci 1993, 50, 699.
37. Houshyar, S.; Shanks, R. A.; Hodzic, A. J Appl Polym Sci 2005, 96, 2260.
38. Amash, A.; Zugenmaier, P. J Appl Polym Sci 1997, 63, 1143.
39. Oksman, K.; Lindberg, H. J Appl Polym Sci 1998, 68, 1845.
40. Nielsen, L. E. Mechanical Properties of Polymers and Composites, Vol. 2; Marcell Dekker: New York, 1974.
41. Manikandan Nair, K. C.; Thomas, S.; Groeninckx, G. Compos Sci Technol 2001, 61, 2519.
42. Qiu, W.; Zhang, F.; Endo, T.; Hirotsu, T. Polym Compos 2005, 26, 448.
43. Ashori, A.; Nourbakhsh, A. J Appl Polym Sci 2009, 111, 2616.
44. Grozdanov, A.; Buzarovska, A.; Bogoeva-Gaceva, G.; Avella, M.; Errico, M. E.; Gentille, G. Agron Sustain Dev 2006, 26, 251.
45. Rosa, S. M. L.; Nachtigall, S. M. B.; Ferreria, C. A. Macromol Res 2009, 17, 8.
46. Herve, E.; Zaoui, A. Eur J Mech A Solids 1990, 9, 505.
47. Herve, E.; Zaoui, A. Int J Eng Sci 1993, 31, 1.
48. Herve, E.; Zaoui, A. Int J Eng Sci 1995, 33, 1419.
49. Jafarzadeh-Dogouri, F. Investigation on Possibility Usage of Recycled Polyethylene Terephthalate in Polypropylene Filled Rice Husk Flour. MSc Dissertation. IPPI: Tehran, Iran, 2006.
50. Klein, N.; Marom, G.; Pegoretti, A.; Migliaresi, C. Composites 1995, 26, 707.
51. Klein, N.; Marom, G. Composites 1994, 25, 706.
52. Scott, G. D. Nature 1960, 188, 908.
53. McGeary, R. K. J Am Ceram Soc 1961, 44, 513.